Electronic supplementary information (ESI)

Amino group dependent sensing property of metal-organic frameworks: Selective turn-on fluorescent detection of lysine and arginine

Jing Dong,[a,b] Xiu-Du Zhang,[a] Xia-Fei Xie,[a] Fan Guo[a] and Wei-Yin Sun*[a]

[a] *Coordination Chemistry Institute, State Key Laboratory of Coordination Chemistry, School of Chemistry and Chemical Engineering, Nanjing National Laboratory of Microstructures, Collaborative Innovation Center of Advanced Microstructures, Nanjing University, Nanjing 210023, China*

[b] *Nanjing Tech University, Nanjing 211816, China*

* Corresponding author.

Email address: sunwy@nju.edu.cn (W. Y. Sun).

Table S1. Comparison of the sensing performance of some reported fluorescent turn-on sensors towards Lysine

Probes	Solvent	Linear range (mM)	K (M^{-1})	LOD (μM)	Reference
UiO-66-NH_2	H_2O	0-3.475	1.81×10^3	60.22	This work
GQD/AuNPs	H_2O/PBS	0.047-0.8	/	16.14	S1
Pyrylium salt	CH_3CN/H_2O	/	/	36.1	S2
8-hydroxypyrene-1,3,6-trisulfonic acid trisodium salt	H_2O	0-0.045	/	3.106	S3
GO-Al-AR	H_2O	0.171-1.71	3.861×10^3	13.68	S4
Pyridinium–Urea-Coupled Polyether	CH_3CN/H_2O/HEPES	/	1.06×10^3	25	S5
CuNCs	H_2O/HAc-NaAc	0.01-1.0	1.098×10^3	5.5	S6
Chiral carbon dots	H_2O/DHP-CA	0-1.0	93.866	3.44	S7
Cd–TCOOH	H_2O/HEPES	0-0.14	/	4	S8

Table S2. Comparison of the sensing performance of some reported fluorescent turn-on sensors towards Arginine

Probes	Solvent	Linear range (mM)	K (M^{-1})	LOD (μM)	Reference
UiO-66-NH_2	H_2O	0-0.645	8.03×10^3	21.50	This work
8-hydroxypyrene-1,3,6-trisulfonic acid trisodium salt	H_2O	0-0.045	/	1.941	S3
hydroxyphenylbenzothiazole (HBT)-based fluorescent probe (HBT-Py)	DMSO	/	/	2.24	S9
GSH-Ag NCs	AA/H_2O	0.01–0.18	/	0.5	S10
1,3,6,8-Tetrakis(p-benzoic acid)pyrene (TBAPy)	H_2O	0–0.2	6.8×10^5	2.3	S11
polydiacetylene vesicles (PDAs)-Mg^{2+}	H_2O	0-0.15	9.1×10^4	4.27	S12
(UO_2)(nip)(2,2′-bpy)	H_2O	0-0.22	3.46×10^3	1.06	S13
dual-emission carbon dots (CDs)	H_2O	0.027-0.107	9.91×10^3	9.16	S14
Au/CQDs composite	H_2O/PBS	0.001–0.005	6.864×10^6	0.45	S15

Table S3. Chemical shifts of Lys and Arg in DCl/DMSO-d_6, UiO-66-NH_2 digested in HF/DMSO-d_6 before and after the immersion in the solution of Lys and Arg.

	δ(ppm)
UiO-66-NH_2	8.05 (s), 7.86 (s), 7.79 (d), 7.36 (d), 7.08 (dd), 2.86 (s), 2.71 (s), 2.10 (s), 1.88 (s)
Lys	8.60 (d), 8.19 (s), 3.80 (t), 2.70 (t), 1.77 (q), 1.52-1.58 (m), 1.39-1.47 (m), 1.28-1.37 (m)
UiO-66-NH_2 + Lys	8.05 (s), 7.79 (d), 7.55 (br), 7.36 (d), 7.10 (dd), 3.80 (s), 2.74-2.80 (m), 2.10 (s), 1.71-1.84 (m), 1.52-1.58 (m), 1.38-1.46 (m), 1.29-1.37 (m)
Arg	3.76 (t), 3.03 (s), 1.72 (d), 1.33-1.57 (m)
UiO-66-NH_2 + Arg	8.06 (s), 7.79 (d), 7.35 (d), 7.09 (dd), 6.70 (br), 3.83 (t), 3.10 (q), 2.10 (s), 1.74-1.87 (m), 1.47-1.66 (m)

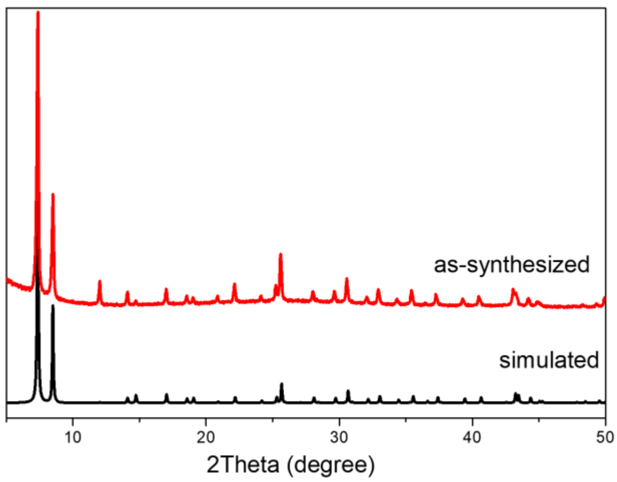

Fig. S1 PXRD patterns of UiO-66-NH_2.

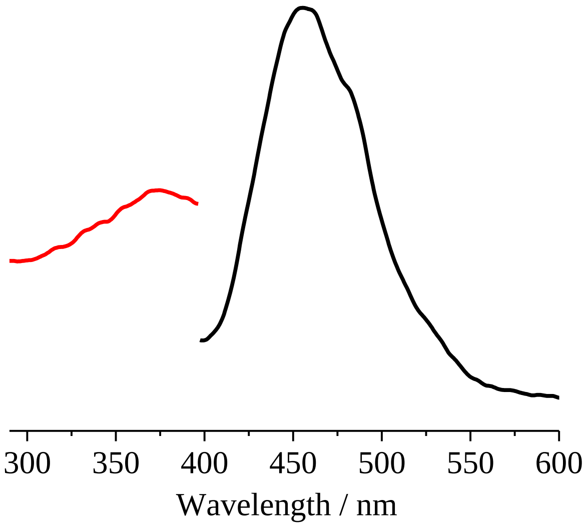

(a)

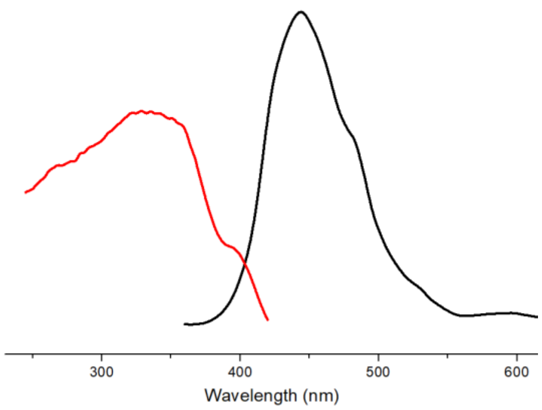

(b)

Fig. S2. The fluorescence excitation and emission spectra of UiO-66-NH_2 in the solid state (a) and the aqueous suspension (b).

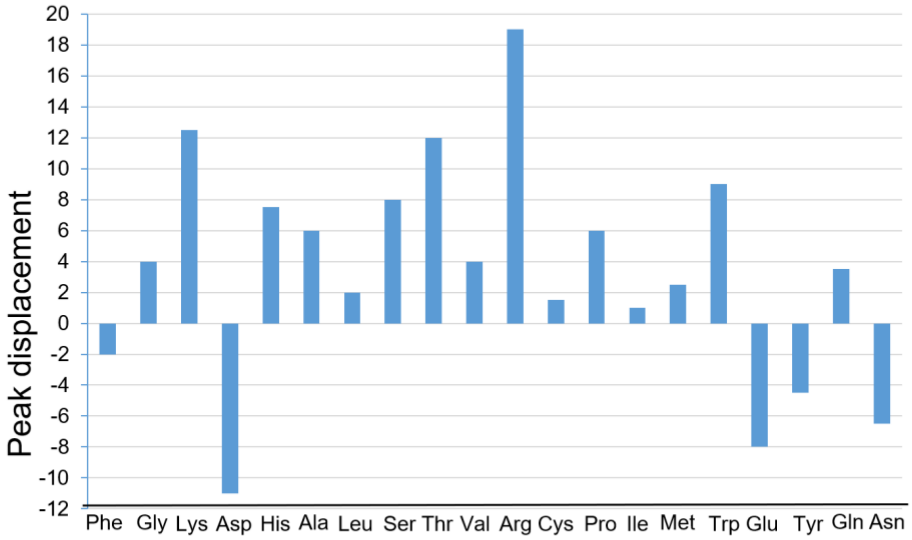

Fig. S3. The maxima wavelength shift of the suspension of UiO-66-NH_2 upon the addition of AAs, positive value refers blue-shift (nm) and negative value presents red-shift (nm).

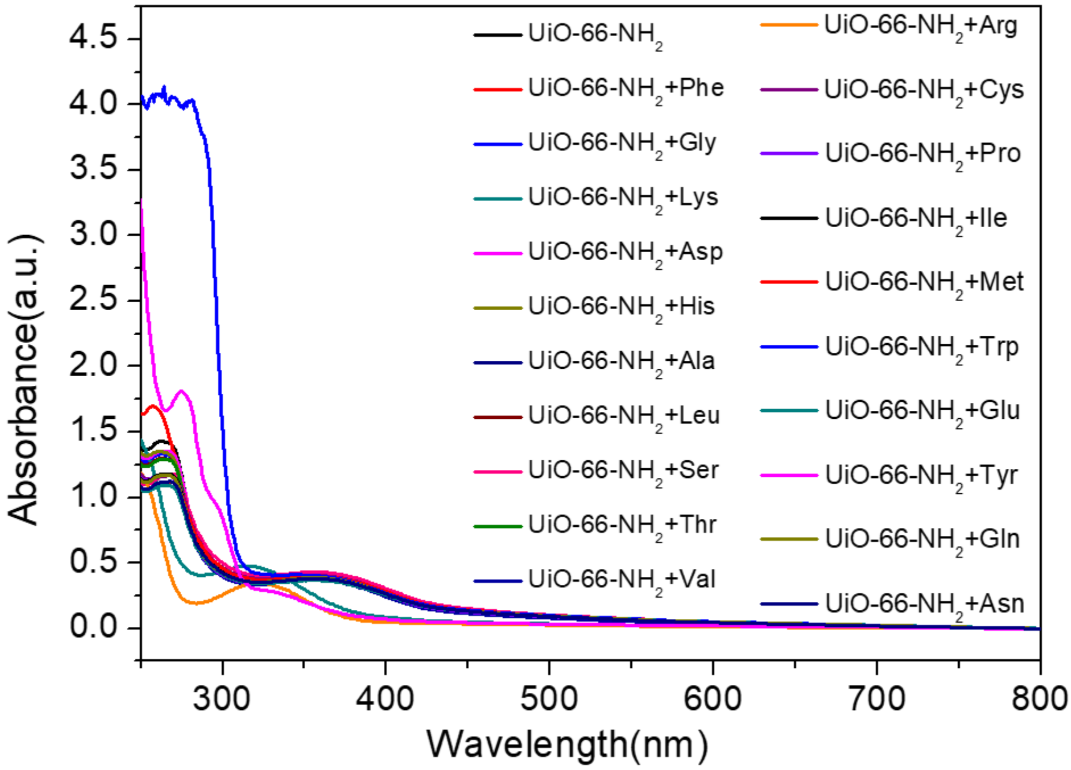

Fig. S4. UV-Vis spectra of the suspension of UiO-66-NH2 with different AAs.

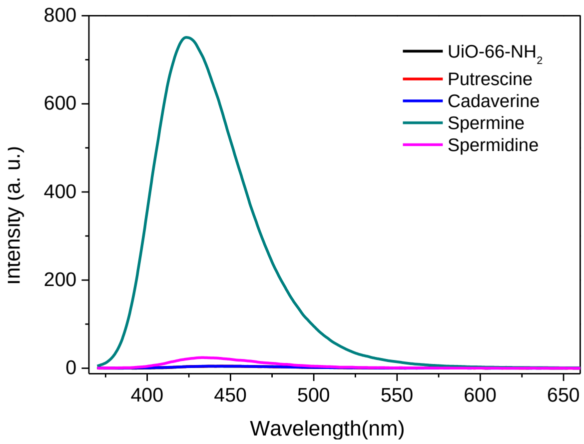

Fig. S5. The fluorescence emission curves of the aqueous suspension of UiO-66-NH2 in the absence and presence of different amines.

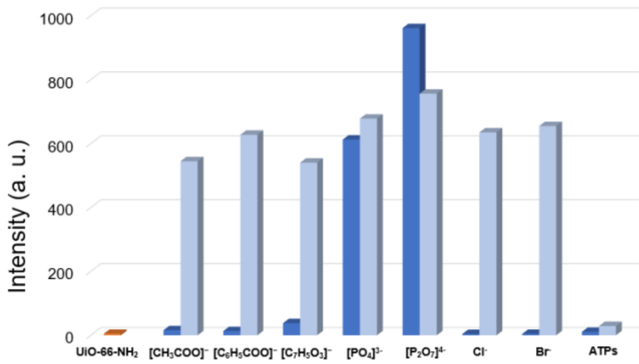

(a)

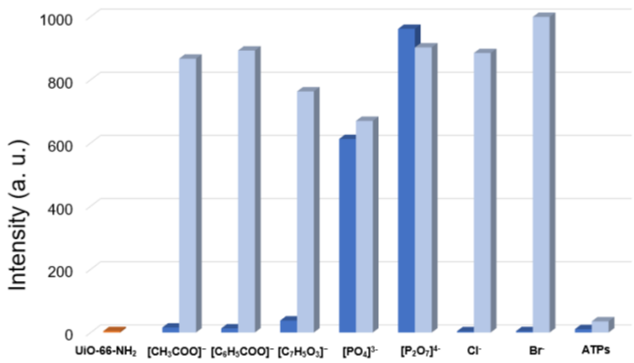

(b)

Fig. S6. Maximum fluorescence intensities of the aqueous suspension of UiO-66-NH_2 by the sequential addition of sodium salt different anions and Lys (a)/Arg (b).

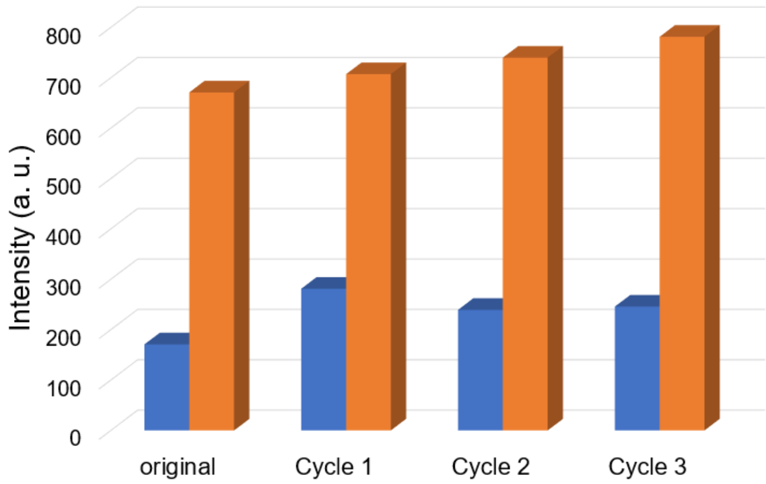

(a)

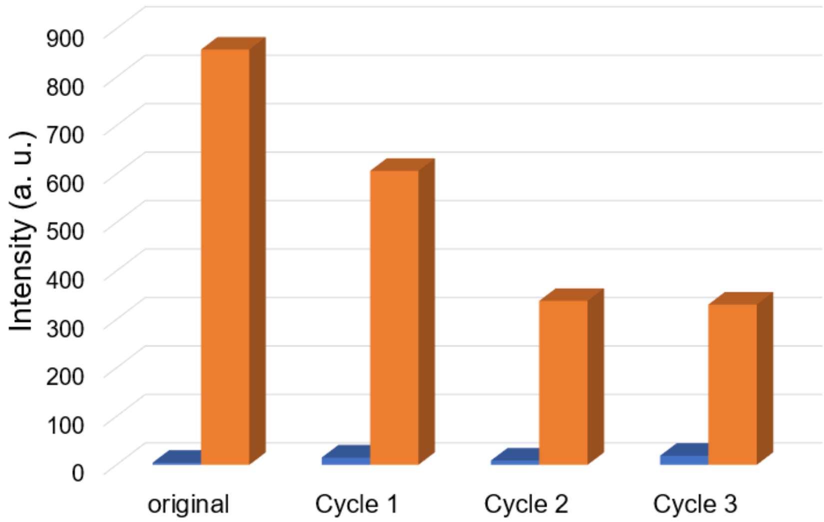

(b)

Fig. S7. Fluorescence enhancement and repeatability tests for Lys (a) and Arg (b).

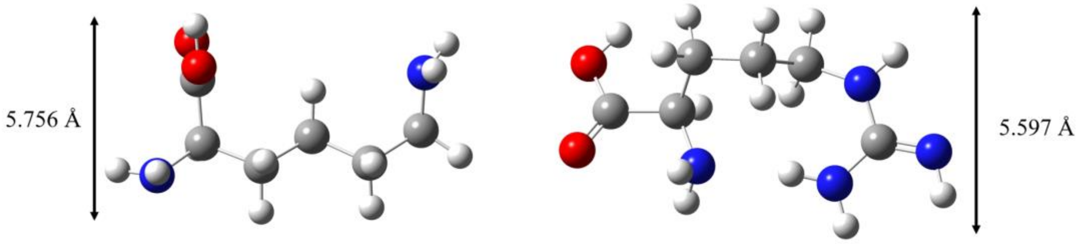

Fig. S8. The longitudinal size of Lys and Arg based on the calculation on Gaussian 09 with b3lyp/6-31g basis sets. The reported internal pore of UiO-66-NH_2 is accessible for guest molecules through triangular windows with size of about 6 Å.

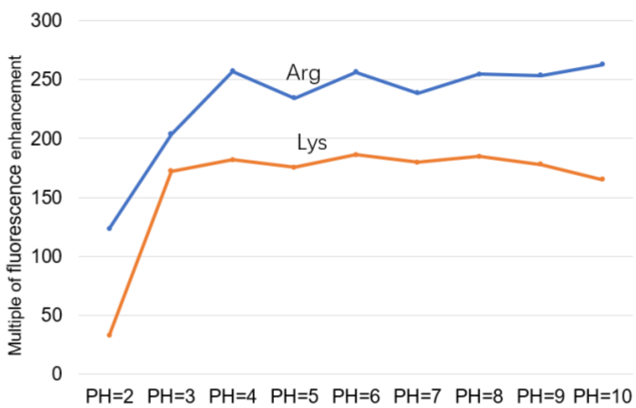

Fig. S9. The emission intensity increments at the maximum wavelength upon the addition of the solution of Lys/Arg (0.5 mL, 0.1 mM) into the suspension of UiO-66-NH_2 (2 mL) under different pH.

References

S1 C. Chaicham, T. Tuntulani, V. Promarak, B. Tomapatanaget, *Sens. Actuators B: Chem.*, 2019, **282**, 936-944.

S2 X. Qian, W. Gong, F. Wang, Y. Lin, G. Ning, *Tetrahedron Lett.*, 2015, **56**, 2764-2767.

S3 R. S. Bhosale, G. V. Shitre, R. Kumar, D. O. Biradar, S. V. Bhosale, R. Narayan, S. V. Bhosale, *Sens. Actuators B: Chem.*, 2017, **241**, 1270-1275.

S4 R. Cheng, H. Huang, Y. Peng, C. Ge, S. Ou, Y. Bu, Y. Xue, H. Liu, L. Dai, *Microchim. Acta*, 2017, **184**, 3521-3528.

S5 K. Ghosh, D. Tarafdar, I. D. Petsalakis, G. Theodorakopoulos, *Eur. J. Org. Chem.*, 2017, **2017**, 355-362.

S6 M. Zhang, J. Qiao, S. Zhang, L. Qi, *Talanta*, 2018, **182**, 595-599.

S7 P. Gao, Z. Xie, M. Zheng, *Sens. Actuators B: Chem.*, 2020, **319**, 128265.

S8 Y. Liu, M Huangfu, P. Wu, M. Jiang, X. Zhao, L. Liang, L. Xie, J. Bai, J. Wang, *Dalton Trans.*, 2019, **48**, 13834-13840.

S9 S. W. Zhang, D. D. Wu, X. Jiang, F. Xie, X. D. Jia, X. L. Song, Y. Yuan, *Sens. Actuator B: Chem.*, 2019, **290**, 691-697.

S10 N. Li, Y. He, Y. Ge, G. Song, *J. Fluoresc.*, 2017, **27**, 293-302.

S11 J. S. Hao, M. Wang, S. T. Wang, Y. Huang, D. P. Cao, *Dyes Pigment.*, 2020, **175**, 108131.

S12 Z. J. Zhang, T. W. Wei, Y. H. Chen, T. T. Chen, B. Chi, F. Wang, X. Q. Chen, *Sens. Actuator B: Chem.*, 2018, **255**, 2211-2217.

S13 L. Wang, B. Tu, W. Xu, Y. Fu, Y. Zheng, *Inorg. Chem.*, 2020, **59**, 5004-5017.

S14 Y. Y. Wang, H. X. Liu, H. H. Song, M. M. Yu, L. H. Wei, Z. X. Li, *New J. Chem.*, 2019, **43**, 13234-13239.

S15 T. Liu, N. Li, J. X. Dong, Y. Zhang, Y. Z. Fan, S. M. Lin, H. Q. Luo, N. B. Li, *Biosens. Bioelectron.*, 2017, **87**, 772–778.